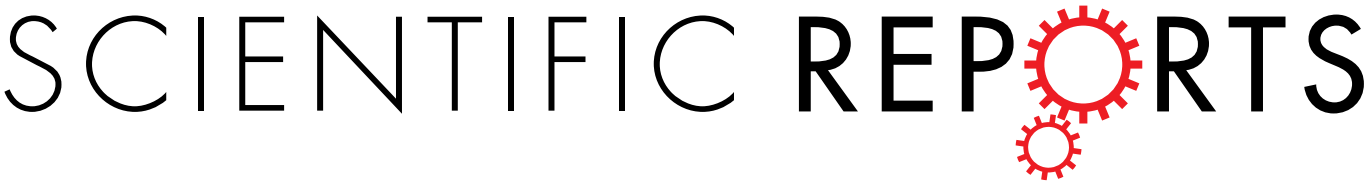

OPEN

H_{18} Carbon: A New Metallic Phase with sp^2-sp^3 Hybridized Bonding Network

Received: 08 October 2015
Accepted: 28 January 2016
Published: 23 February 2016

Chun-Xiang Zhao[1], Chun-Yao Niu[1,2], Zhi-Jie Qin[1], Xiao Yan Ren[1], Jian-Tao Wang[3], Jun-Hyung Cho[4,2] & Yu Jia[1,2]

Design and synthesis of three-dimensional metallic carbons are currently one of the hot issues in contemporary condensed matter physics because of their fascinating properties. Here, based on first-principles calculations, we discover a novel stable metallic carbon allotrope (termed H_{18} carbon) in *P6/mmm* (D_{6h}^{1}) symmetry with a mixed sp^2-sp^3 hybridized bonding network. The dynamical stability of H_{18} carbon is verified by phonon mode analysis and molecular dynamics simulations, and its mechanical stability is analyzed by elastic constants, bulk modulus, and shear modulus. By simulating the x-ray diffraction patterns, we propose that H_{18} carbon would be one of the unidentified carbon phases observed in recent detonation experiments. The analysis of the band structure and density of states reveal that this new carbon phase has a metallic feature mainly due to the C atoms with sp^2 hybridization. This novel 3D metallic carbon phase is anticipated to be useful for practical applications such as electronic and mechanical devices.

Carbon has a variety of structural allotropes due to its ability of different hybridizations[1]. It is well known that there exist three carbon allotropes in natural materials, that is, graphite, diamond, and amorphous carbon, containing the sp^2, sp^3, and mixed sp^2/sp^3 hybridized carbon atoms[2], respectively. In the past three decades, intensive theoretical and experimental efforts have been focused on synthesizing new allotropes of carbon, among which, the zero-dimensional (0D) fullerenes[3], one-dimensional (1D) carbon nanotubes[4], and two-dimensional (2D) graphene[5] are the three most prototypical examples. So far, many new carbon allotropes such as 1D *sp*-carbyne, 2D *sp*-sp^2-graphyne, and three-dimensional (3D) *sp*-sp^3-yne-diamond have been experimentally fabricated or theoretically predicted[6,7], most of them exhibit their intriguing mechanical and electronic properties. Recently, a new carbon allotrope with hardness even higher than diamond has also been observed by compressing graphite with pressure over 17 GPa[8]. Motivated by this experimental finding, several carbon crystalline phases such as monoclinic *M*-carbon[9], bct-C_4 carbon[10], *W*-carbon[11], *O*-carbon[12], and *Z*-carbon[13] were proposed to simulate this high-pressure carbon phase. These prototypical examples have given rise to significant impacts in material and information sciences, stimulating experimental and theoretical attentions on carbon allotropes[14–23].

Among various types of carbon materials, metallic carbon allotropes exhibit more fascinating properties, e.g., a highly efficient catalytic property due to its high electronic density of states (DOS) at the Fermi level[24]. It was also identified that metallic carbon becomes magnetic when the Stoner-like criterion[25,26] is satisfied. Furthermore, metallic carbon showed a number of intriguing properties such as phonon-plasmon coupling[27], superconductivity[28,29] and negative differential resistance[30]. Consequently, the exploration of metallic carbon candidates have attracted considerable attention in the synthesis and design of new carbon allotropes. However, all of the 3D carbon allotropes mentioned above are semiconductors or insulators.

There have so far been few progresses in search of 3D metallic carbon. Some hypothetical 3D carbon allotropes such as $ThSi_2$-type tetragonal carbon[31], hexagonal H-6 carbon[32], and K_4 carbon[33] have been proposed to be metallic. However, all of such structures were found to be dynamically unstable[19,34,35]. In 2012, a simple cubic phase of carbon was reported to be metallic under 3 TPa, but it becomes unstable when pressure is removed[36].

[1]International Laboratory for Quantum Functional Materials of Henan, and School of Physics and Engineering, Zhengzhou University, Zhengzhou 450001, China. [2]Center for Advanced Analysis and Computional Science, Zhengzhou University, Zhengzhou 450001, China. [3]Beijing National Laboratory for Condensed Matter Physics, Institute of Physics, Chinese Academy of Sciences, Beijing 100190, China. [4]Department of Physics and Research Institute for Natural Sciences, Hanyang University, 17 Haengdang-Dong, Seongdong-Ku, Seoul 133-791, Korea. Correspondence and requests for materials should be addressed to C.Y.N. (email: niuchunyao@zzu.edu.cn)

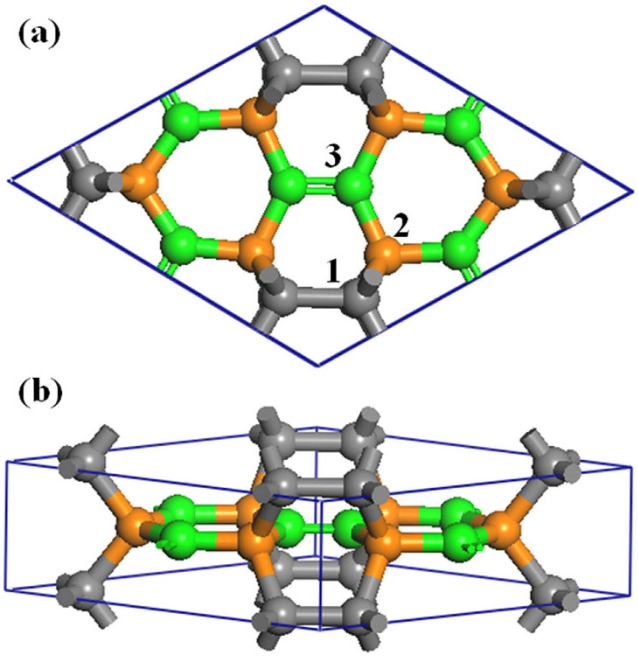

Figure 1. Top (**a**) and side (**b**) views of H_{18} carbon in $P6/mmm$ (D_{6h}^1) symmetry with single and double bonds. The carbon atoms on 6*l* (0.2579, 0.1289, 0), 6 m (0.583, 0.7915, 0.5), and 6 m (0.8933, 0.4467, 0.5) Wyckoff positions are denoted by C_1 (gray), C_2 (orange) and C_3 (green), respectively.

Recently, a 3,4-connected T6 carbon allotrope was proposed to be metallic, but it was also unstable at temperature about 500 K[37]. More recently, a 3D metallic K_6 carbon with pure sp^3 hybridization was reported to have a high DOS at the Fermi level[38], however, its stability is too low to be synthesized. To our knowledge, all of these theoretical predictions of 3D metallic carbon allotropes have not been experimentally realized so far.

Here, based on first-principles total-energy and phonon calculations[39–46], we discover a new stable 3D metallic carbon allotrope in $P6/mmm$ (D_{6h}^1) symmetry with a mixed sp^2-sp^3 hybridized bonding network. This new phase is composed of eighteen atoms per hexagonal primitive cell (hereafter termed H_{18} carbon), having a larger atom density of 3.135 g/cm^3 compared to 2.28 g/cm^3 for graphite. The calculated elastic constants show that the H_{18} carbon is a brittle material. From the analysis of the phonon spectra, we find that H_{18} carbon does not have any unstable vibration modes. Interestingly, the simulated x-ray diffraction (XRD) pattern of H_{18} carbon matches one of the unidentified carbon phases observed in recent detonation experiments[47]. The calculated band structure and DOS of H_{18} carbon manifest a metallic feature mainly due to the C atoms with sp^2 hybridization. The H_{18} carbon has great potential application in electronics, mechanics, and some other related fields due to its novel properties.

Results

Figure. 1 shows the structure of H_{18} carbon with a 3D sp^2-sp^3 hybridized bonding network in $P6/mmm(D_{6h}^1)$ symmetry. Here, the hexagonal primitive cell contains eighteen C atoms with equilibrium lattice parameters a = b = 7.125 Å, c = 2.605 Å. The C_1, C_2, and C_3 atoms in Fig. 1 are bonded to four, four, and three neighboring carbon atoms, thus forming sp^3, sp^3 and sp^2 bonds, respectively. The calculated bond lengths $d_{C_1-C_1}$, $d_{C_1-C_2}$, $d_{C_2-C_3}$, and $d_{C_3-C_3}$ are 1.591, 1.631, 1.475, and 1.317 Å, respectively. Note that $d_{C_2-C_3}$ is between the bond lengths (1.420 and 1.544 Å) of graphite and diamond which have sp^2 and sp^3 bonds, respectively. Because of a mixed bonding of sp^3 and sp^2, H_{18} carbon has five different bond angles of 107.5°, 110.1°, 110.4°, 115.2° and 129.6°, contrasting with 109.5° for sp^3 hybridized diamond and 120° for sp^2 hybridized graphite. Such several bond distortions in H_{18} carbon implies the presence of strain, leading to a decrease of the relative stability compared to diamond and graphite as discussed below. In Table 1, we list the calculated lattice parameters, equilibrium densities, bond lengths, and cohesive energies of diamond, graphite, Rh6, T6, BC8, and H_{18} carbons. We find that our results agree well with previous DFT calculations and experiments[21,22,37]. We note that the equilibrium bulk atom density of H_{18} carbon is 3.135 g/cm^3, larger than that (2.28 g/cm^3) of graphite[21].

In order to check the stability of H_{18} carbon, we perform the analyses of total energy, phonon mode, and elastic constants as well as molecular dynamic (MD) simulations.

(i) *Total energy*: Figure 2 shows the calculated total energies of H_{18} carbon, diamond, graphite, BC8, T6 and Rh6 carbon as a function of volume per atom. It is seen that graphite and diamond are more thermodynamically stable than H_{18} carbon as well as other carbon phases. We note, however, that H_{18} carbon is not only much more stable than BC8 carbon (which has been suggested to be the derivative of cubic diamond under pressure of ~1100 GPa[48–50]), but also more stable than T6 carbon and Rh6[20,37]. In particular, H_{18} carbon has a relatively

Structure	Space group	Method	a (Å)	c (Å)	ρ (g/cm^3)	d (Å)	E_{coh} (eV/atom)
Diamond	$Fd\bar{3}m$	LDA	3.535		3.611	1.531	8.927
		PBE	3.572		3.501	1.578	7.780
		Exp.[22]	3.567		3.520	1.544	
Graphite	$P6_3/mmc$	LDA	2.446	6.594	2.335	1.412	8.918
		PBE	2.467	8.145	1.859	1.424	7.900
		Exp.[21]	2.460	6.704	2.280	1.420	
T6	$P4_2/mmc$	LDA	2.567	5.937	3.059	1.522, 1.331	8.416
		PBE[37]	2.600	6.000	2.952	1.540, 1.340	
BC8	$Ia\bar{3}$	LDA	4.426		3.681	1.446, 1.611	8.239
		PBE	4.477		3.556	1.456, 1.631	7.082
Rh6	$R\bar{3}m$	LDA	6.914	3.277	2.647	1.469, 1.357	8.441
		PBE	6.885	3.585	2.439	1.491, 1.357	7.400
H_{18}	$P6/mmm$	LDA	7.056	2.563	3.248	1.310–1.609	8.547
		PBE	7.125	2.605	3.135	1.317–1.631	7.269

Table 1. Calculated lattice parameters a and c (in Å), equilibrium density (ρ in g/cm^3), bond length (d in Å) and cohesive energy (E_{coh} in eV) of H_{18} carbon in comparison with those of diamond, graphite and some other carbon allotropes.

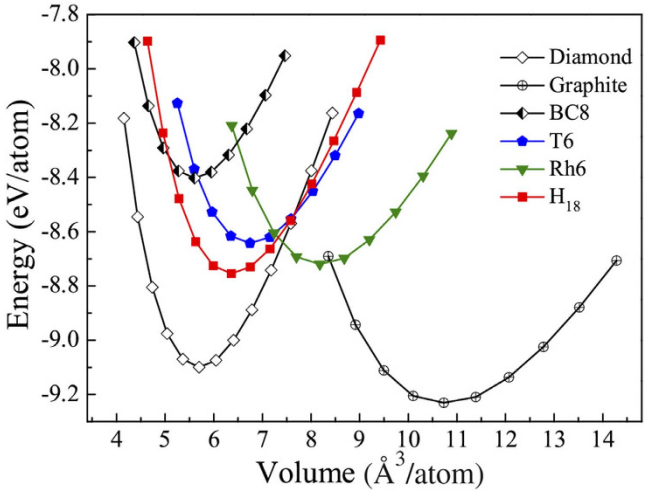

Figure 2. Total energy of H_{18} carbon as a function of volume per atom in comparison with those of diamond, graphite, BC8, T6, and Rh6 carbon (GGA-PBE calculations).

smaller 18-atom hexagonal unit cell compared to Rh6 (see Fig. 2). From the energy-volume curves of carbon allotropes (Fig. 2), one expects that Rh6 carbon can be transformed into H_{18} carbon by applying a certain pressure.

(ii) *Phonon mode*: The calculated phonon band structure and DOS are displayed in Fig. 3. It is found that there is no negative frequencies throughout the entire Brillioun zone, indicating the dynamical stability of H_{18} carbon. In Fig. 3, the highest vibrational frequency of H_{18} carbon amounts to $\sim$1837 cm^{-1} at A point, which is higher than $\sim$1400 cm^{-1} of the perfectly sp^3 bonded diamond[51] as well as $\sim$1600 cm^{-1} of the π-conjugated graphite[52]. We note that there exists a wide band gap of $\sim$230 cm^{-1} between 1449 and 1679 cm^{-1} near the K point. These features of phonon spectra of H_{18} carbon are anticipated to be measured by future experiments. In Fig. 3, we also plot the atom-resolved phonon DOS contributed by C_1, C_2 and C_3 atoms, respectively. Obviously, the highest frequency modes around 1750 cm^{-1} originate from the vibrations of the strong sp^2 C_3-C_3 bonds with a bond length of 1.317 Å, while the second highest frequency modes around 1450 cm^{-1} arise from the mixed sp^2-sp^3 C_2-C_3 bonds with a bond length of 1.475 Å. These characters of H_{18} carbon are different from both graphite with bond length of 1.420 Å and diamond with bond length of 1.544 Å.

(iii) *Elastic constants:* In the linear elastic regime, the elastic constant tensor is constituted a symmetric 6×6 matrix with 21 independent components, where only C_{11}, C_{12}, C_{13}, C_{33} and C_{44} are independent in the hexagonal lattice[53]. According to the Born stability conditions[53], the elastic constants of the hexagonal lattice should satisfy $C_{11}>|C_{12}|$, $C_{44}>0$, $C_{66}>0$, and $2C_{13}^2<C_{33}(C_{11}+C_{12})$. The calculated elastic constants of H_{18} carbon as well as diamond, T6, BC8, and Rh6 carbons are listed in Table 2. Specifically, the calculated elastic constants C_{ij} of H_{18}

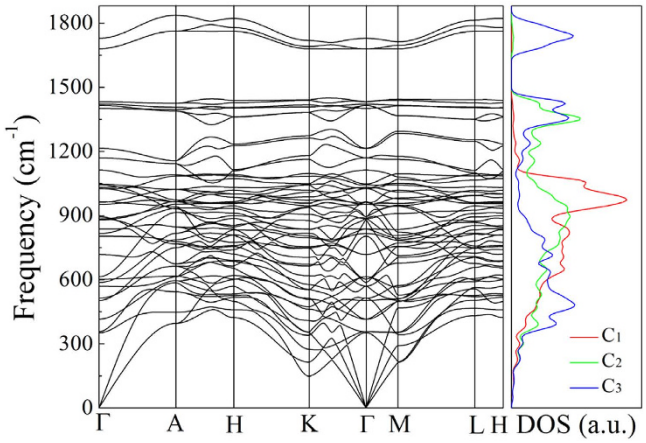

Figure 3. Calculated phonon band structures and density of states (DOS) of H_{18} carbon using the LDA calculations.

Structure	C_{11}	C_{12}	C_{13}	C_{33}	C_{44}	C_{66}	B	G	B/G
Diamond[23]	1055	126			565		435	522	0.83
T6[37]	730	25	89	1165	81	68	337	197	1.71
BC8	1172	54			559		427	559	0.76
Rh6	735	152	161	175	218		231	188	1.23
H_{18}	1233	104	16	667	214		360	361	1.00

Table 2. Calculated elastic constants C_{ij} (GPa), bulk modulus B (GPa), shear modulus G (GPa) and B/G value for H_{18} carbon in comparison with diamond, T6, BC8, and Rh6 carbon.

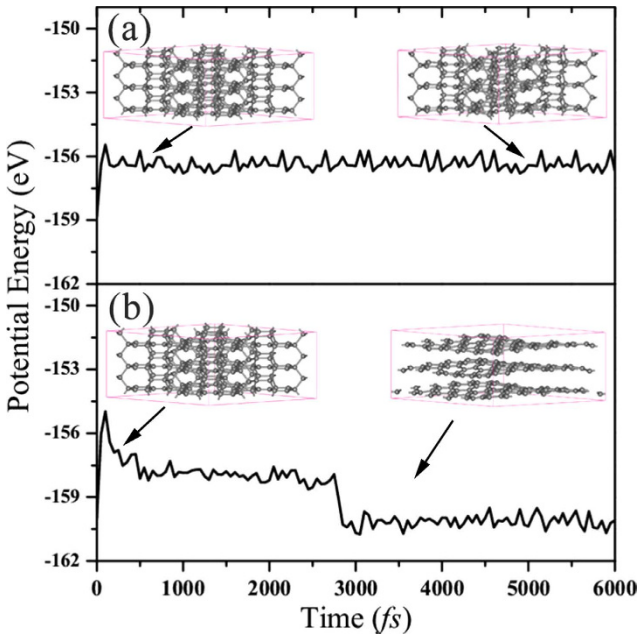

Figure 4. Potential energy fluctuation of H_{18} carbon in MD simulation at 1000 K (**a**) and 1500 K (**b**). (Inset) Snapshots depict the process of phase transition.

carbon satisfy well all of the conditions, indicating that the structure of H_{18} carbon is mechanically stable. The bulk modulus and shear modulus obtained by Voigt-Reuss-Hill approximation[54] are also listed in Table 2. The magnitude of the bulk modulus of H_{18} carbon is fairly large as 360 GPa, which amounts to about four fifths of that (435 GPa) of diamond and even larger than that (337 GPa) of T6 carbon[37]. This result indicates that H_{18} carbon is more resistant to hydrostatic compression compared to T6 carbon. The B/G ratio of H_{18} carbon is about 1.0, close

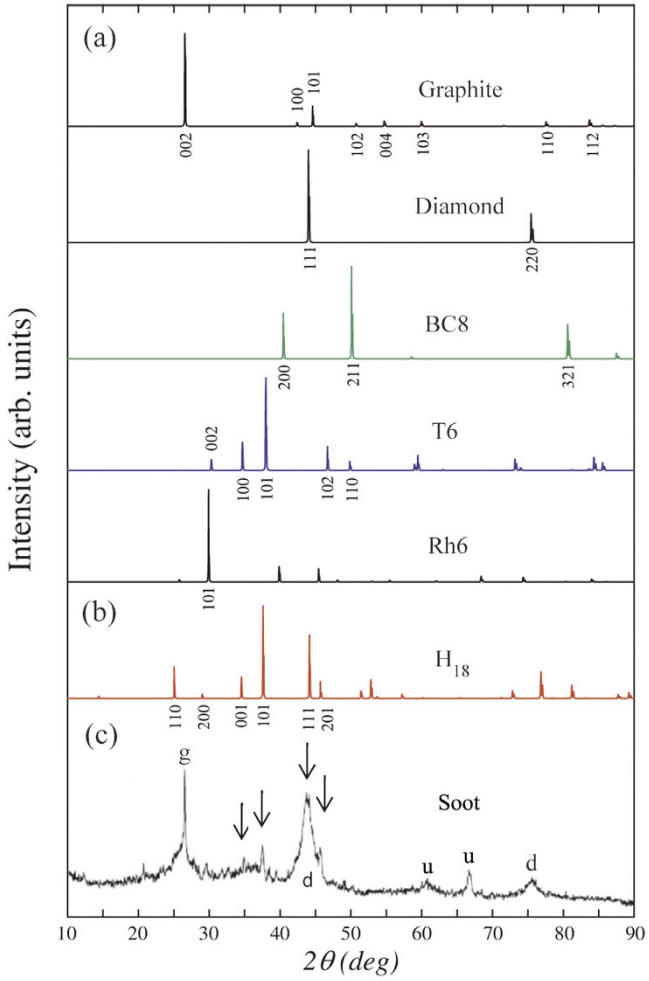

Figure 5. Comparison of simulated and experimental X-ray diffraction (XRD) patterns. (a) Simulated XRD patterns for graphite, diamond, BC8, T6 and Rh6 carbon. **(b)** Simulated XRD patterns for H_{18} carbon. **(c)** Experimental XRD patterns for detonation soot (sample Alaska C)[47]. *g*, *d*, *u* indicate graphite, diamond, unknown-carbon, respectively. The X-ray wavelength we adopted is 1.54059 Å.

to that (0.83) of diamond, implying that H_{18} carbon can be characterized as a brittle material according to the Paugh criterion[55].

(iv) *MD simulations*: To examine the thermal stability of H_{18} carbon, we carried out the ab initio MD simulations with the canonical (NVT) ensemble at temperature of 300, 1000 and 1500 K, respectively. The system is modeling with a $2 \times 2 \times 3$ supercell containing 216 carbon atoms and the time step of 1 fs is used. The potential energy fluctuation of H_{18} carbon in MD simulation at 1000 and 1500 K are presented in Fig. (4a,b), respectively. We can see that the potential energy fluctuation are very small and geometry of H_{18} carbon remains intact after heating up to 1000 K for 6 picoseconds. With the temperature increasing up to 1500 K, we find that the H_{18} carbon becomes graphitization gradually (see in Fig. (4b)). These results have indicated that H_{18} carbon, once synthesized, can sustain the structure even at temperature of 1000 K. For comparison, Ab initio MD simulations for T6 carbon with the same setting and a $2 \times 4 \times 4$ supercell containing 192 carbon atoms show that it is unstable even at 500 K[37]. Based on our MD simulations, we can say that H_{18} carbon is much more stable than T6 carbon at high temperature.

In addition, to evidence the experimental observation of H_{18} carbon, we plot the simulated XRD spectra of graphite, diamond, BC8, T6, Rh6, and H_{18} carbons in Fig. 5(a,b), together with the experimental XRD data of TNT/RDX detonation soot in Fig. 5(c). In the experimental XRD data[47], the diffraction lines arising from graphite (*g*), diamond (*d*), and other unknown (*u*) carbon phases were reported. As shown in Fig. 5(b,c,i) the (001), (101) and (201) peaks of H_{18} carbon match well with the experimental XRD spectra located at 34.4°, 37.4° and 45.5°, respectively, and (ii) the (111) peak of H_{18} carbon that overlaps with the (111) peak of diamond can be associated with the second-strongest experimental XRD peak at 43.9°. Meanwhile, the (110) and other peaks of H_{18} carbon can not be clearly identified in the experimental XRD patterns, but may be overlapped with neighboring peaks of other carbon phases. Note that the position of (100) and (101) peaks of T6 are very close to the position of (001) and (101) peaks of H_{18} carbon, respectively. Since H_{18} carbon is thermodynamically more stable than T6 carbon as mentioned above, it is most likely that the experimental XRD peaks near 34° and 37° would be predominantly

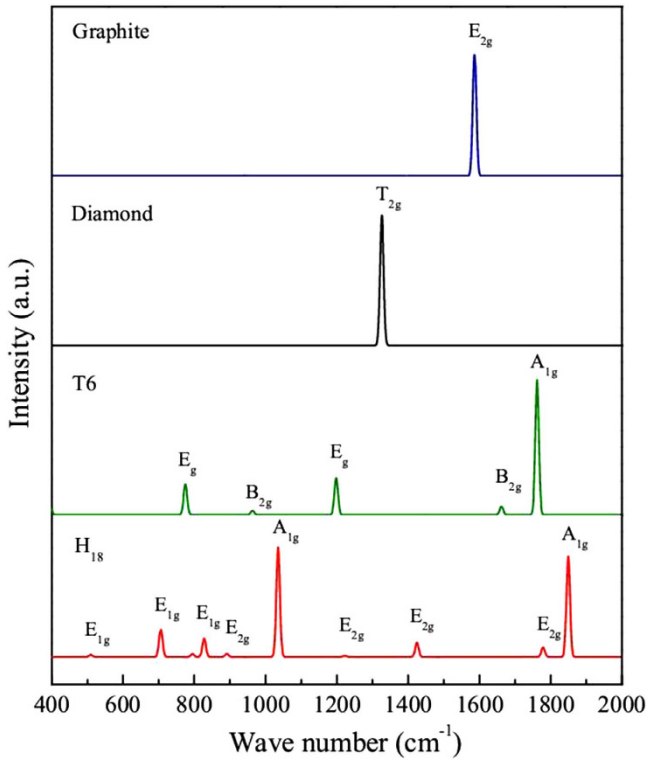

Figure 6. Comparison of simulated Raman spectra for H_{18}, graphite, diamond and T6.

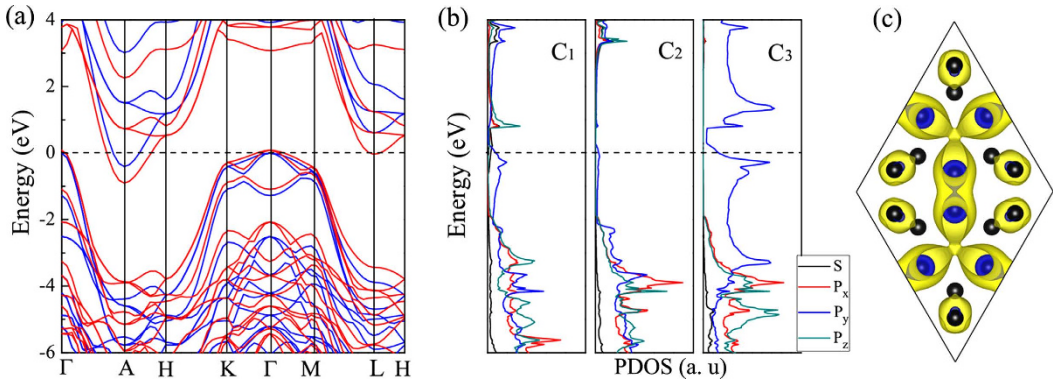

Figure 7. Electronic band structures, density of states and decomposed charge density of H_{18} carbon. **(a)** Electronic band structures calculated using GGA-PBE (red lines) and HSE06 hybrid functional (blue lines). **(b)** The projected density of states (PDOS) for C_1, C_2, and C_3 atom at GGA-PBE level. The Fermi level is set at 0 eV. **(c)** The charge density isosurfaces (0.01 e/Å^3) of the partially occupied band of H_{18} carbon.

associated with H_{18} carbon rather than T6 carbon. Therefore, we propose that H_{18} carbon is one of the unidentified carbon phases which were explicitly present in recent detonation experiments[47].

To provide more physical quantities that are accessible from experiments, we also simulated the Raman spectra of H_{18} carbon and compared the results with graphite, diamond and T6 carbon structures. The simulation results are presented in Fig. 6. From Fig. 6, we can see that the E_{2g} mode in graphite is estimated to be 1586 cm^{-1}, which is well agreement with the experimental data of 1581 cm^{-1} [56]. The T_{2g} mode in diamond is estimated to be 1326 cm^{-1}, which is close to the experimental data of 1333 cm^{-1} [57]. Although the main XRD peaks of T6 and H_{18} carbon are close to each other, their Raman spectra show rather different characters. For T6 carbon, there is only one main peak A_{1g} presents at 1762 cm^{-1}. However, we find that, for H_{18}, there are two main peaks A_{1g} at 1035 and 1849 cm^{-1}, respectively. In addition, both T6 and H_{18} carbon also show some weaker peaks (E_g and B_{2g} for T6, E_{1g} and E_{2g} for H_{18}). All the features above may be helpful for identifying this new carbon phase in further experiments.

Finally, we discuss the electronic properties of H_{18} carbon. The band structures and partial density of states (PDOS) are displayed in Fig. 7(a,b), respectively. It is seen that the Fermi level crosses the bands near the A and Γ points, giving rise to the presence of the electron (hole) pocket around A (Γ). Thus, H_{18} carbon is metallic. It is noted that the metallic feature obtained using the semilocal DFT calculation with the Perdew-Burke-Ernzerhof (PBE) functional is preserved in the hybrid DFT calculation with the Heyd, Scuseria, and Ernzerhof (HSE06) functional[58,59] [see Fig. 7(a)]. From the PDOS projected onto C_1, C_2 and C_3 atoms [Fig. 7(b)], we find that the electronic states near E_F dominantly involve the p_y character of C_3. In order to elucidate the origin of the metallic feature in H_{18} carbon, we calculate the charge density of the partially occupied bands in the energy windows of $E_F - 0.5$ to $E_F + 0.5$ eV [see Fig. 7(c)]. It is seen that the p_y orbital of C_3 atoms largely contribute to the charge density, forming a delocalized network. On the basis of the PDOS [Fig. 7(b)] and the charge character near E_F [Fig. 7(c)], we can say that the metallicity of H_{18} carbon is attributed to a large delocalization of the p_y orbital of C_3 atoms with sp^2 hybridization.

Conclusion

Our first-principles DFT total energy and phonon calculations discover a novel stable carbon allotrope (termed H_{18} carbon) which is metallic. The analyses of the total energy, phonon mode, and elastic constants as well as molecular dynamic simulations obviously show that this new carbon allotrope exists as a stable structure. More importantly, we demonstrate that the H_{18} carbon may be one of the candidates of the unidentified carbon phases which appeared in the XRD spectrum analysis of a recent detonation experiment. In particular, H_{18} carbon has a metallic feature mainly due to the p_y orbitals of sp^2 hybridized carbon atoms. Unlike previously reported 3D metallic carbon allotropes, H_{18} carbon can not only keep its metallicity at ambient pressure but also can likely maintain its structure at high temperatures. This novel 3D metallic carbon phase is anticipated to be useful for practical applications such as electronics and mechanics devices. Our findings will attract immediate broad interest and stimulate further experimental and theoretical studies for this new carbon allotrope.

Methods

The present total-energy and phonon calculations were carried out by using the density functional theory. Both local density approximation (LDA) in the form of Ceperley-Alder[39] and the generalized gradient approximation (GGA) developed by Perdew, Burke, and Ernzerhof (PBE)[40] are adopted for the exchange-correlation potential as implemented in the Vienna *ab initio* simulation package (VASP)[41–43]. All the discussions in this paper are based on the results got by GGA-PBE method, except for special notations. The all-electron projector augmented wave (PAW)[44] method is adopted with C $2s^2 2p^2$ treated as valence electrons. A plane-wave basis set with an energy cutoff of 800 eV is used. The Gaussian smearing with a smearing factor of 0.05 eV is used in the calculations. The Brillouin zone (BZ) is sampled by a $9 \times 9 \times 21$ Monkhorst-Pack (MP) special k-point grid including Γ-point. The geometries are optimized with no symmetry constraints, the convergence criteria employed for both the electronic self-consistent relaxation and the ionic relaxation are set to 10^{-7} eV and 10^{-3} eV/Å for electronic energy and Hellmann-Feynman force, respectively. Phonon dispersion curves are calculated by using the package phonopy[45,46] with the forces calculated with VASP code. The first-principles molecular dynamics simulations are performed in the canonical (NVT) ensemble with the Nosé thermostat[60]. Each simulation lasted for 6 ps, with a time step of 1 fs. All the calculations in this work are performed at zero pressure.

References

1. Miller, E. D., Nesting, D. C. & Badding, J. V. Quenchable Transparent Phase of Carbon. *Chem. Mater.* **9,** 18–22 (1997).
2. Balaban, A. T. Carbon and its nets. *Computers Math. Applic.* **17,** 397–416 (1989).
3. Kroto, H. W., Heath, J. R., Obrien, S. C., Curl, R. F. & Smaliey, R. E. C_{60}: Buckminsterfullerene. *Nature* (London) **318**, 162–163 (1985).
4. Iijima, S. Helical microtubules of graphitic carbon. *Nature* (London) **354,** 56–58 (1991).
5. Novoselov, K. *et al.* Electric field effect in atomically thin carbon films. *Science* **306,** 666–669 (2004).
6. Diederich, F. & Kivala, M. All-carbon scaffolds by rational design. *Adv. Mater.* **22,** 803–812 (2010).
7. Hirsch, A. The era of carbon allotropes. *Nature Mater.* **9,** 868–871 (2010).
8. Mao, W. L. *et al.* Bonding changes in compressed superhard graphite. *Science* **302,** 425–427 (2003).
9. Li, Q. *et al.* Superhard monoclinic polymorph of carbon. *Phys. Rev. Lett.* **102,** 175506 (2009).
10. Umemoto, K., Wentzcovitch, R. M., Saito, S. & Miyake, T. Body-centered tetragonal C_4: A viable sp^3 carbon allotrope. *Phys. Rev. Lett.* **104,** 125504 (2010).
11. Wang, J. T., Chen, C. F. & Kawazoe, Y. Low-temperature phase transformation from graphite to sp^3 orthorhombic carbon. *Phys. Rev. Lett.* **106,** 075501 (2011).
12. Wang, J. T., Chen, C. F. & Kawazoe, Y. Orthorhombic carbon allotrope of compressed graphite: *Ab initio* calculations. *Phys. Rev. B* **85,** 033410 (2012).
13. Zhao, Z. S. *et al.* Novel superhard carbon: C-centered orthorhombic C_8. *Phys. Rev. Lett.* **107,** 215502 (2011).
14. Wang, J. T., Chen, C. F., Wang, D. S., Mizuseki, H. & Kawazoe, Y. Phase stability of carbon clathrates at high pressure. *J. Appl. Phys.* **107,** 063507 (2010).
15. Wang, J. T., Chen, C. F. & Kawazoe, Y. New cubic carbon phase via graphitic sheet rumpling. *Phys. Rev. B* **85,** 214104 (2012).
16. Sheng, X. L., Yan, Q. B., Ye, F., Zheng, Q. R. & Su, G. T-carbon: A novel carbon allotrope. *Phys. Rev. Lett.* **106,** 155703 (2011).
17. Wang, X. Q., Li, H. D. & Wang, J. T. Prediction of a new two-dimensional metallic carbon allotrope. *Phys. Chem. Chem. Phys.* **15,** 2024–2030 (2013).
18. Wang, J. T., Chen, C. F. & Kawazoe, Y. Phase conversion from graphite toward a simple monoclinic sp^3-carbon allotrope. *J. Chem. Phys.* **137,** 024502 (2012).
19. Wang, J. T., Chen, C. F. & Kawazoe, Y. New carbon allotropes with helical chains of complementary chirality connected by ethene-type π-conjugation. *Sci. Rep.* **3,** 03077 (2013).
20. Wang, J. T., Chen, C. F., Wang E. G. & Kawazoe, Y. A new carbon allotrope with six-fold helical chains in all-sp^2 bonding networks. *Sci. Rep.* **4,** 04339 (2014).

21. Furthmüller, J., Hafner, J. & Kresse, G. *Ab initio* calculation of the structural and electronic properties of carbon and boron nitride using ultrasoft pseudopotentials. *Phys. Rev. B* **50,** 15606 (1994).
22. Occelli, F., Loubeyre, P. & Letoullec, R. Properties of diamond under hydrostatic pressures up to 140 GPa. *Nature Mater.* **2,** 151–154 (2003).
23. Grimsditch, M. & Ramdas, A. K. Brillouin scattering in diamond. *Phys. Rev. B* **11,** 3139 (1975).
24. Bergeret, C., Cousseau, J., Fernandez, V., Mevellec, J. Y. & Lefrant, S. Spectroscopic evidence of carbon nanotubes metallic character loss induced by covalent functionalization via nitric acid purification. *J. Phys. Chem. C* **112,** 16411–16416 (2008).
25. Ohldag, H. *et al.* π-electron ferromagnetism in metal-free carbon probed by soft x-ray dichroism *Phys. Rev. Lett.* **98,** 187204 (2007).
26. Peng, H. W. *et al.* Origin and enhancement of hole-induced ferromagnetism in first-row d^0 semiconductors *Phys. Rev. Lett.* **102,** 017201 (2009).
27. Piscanec, S., Lazzeri, M., Robertson, J., Ferrari, A. C. & Mauri, F. Optical phonons in carbon nanotubes: Kohn anomalies, peierls distortions, and dynamic effects. *Phys. Rev. B* **75,** 035427 (2007).
28. Terrones, H. *et al.* New metallic allotropes of planar and tubular carbon. *Phys. Rev. Lett.* **84,** 1716 (2000).
29. Kociak, M. *et al.* Superconductivity in ropes of single-walled carbon nanotubes. *Phys. Rev. Lett.* **86,** 2416 (2001).
30. Ni, Y. *et al.* The transport properties and new device design: the case of 6,6,12-graphyne nanoribbons. *Nanoscale.* **5,** 4468 (2013).
31. Hoffmann, R., Hughbanks, T., Kertesz, M. & Bird, PH. A hypothetical metallic allotrope of carbon. *J. Am. Chem. Soc.* **105,** 4831–4832 (1983).
32. Tamor, M. A. & Hass, K. C. Hypothetical superhard carbon metal. *J. Mater. Res.* **5,** 2273C2276 (1990).
33. Itoh, M. *et al.* New Metallic Carbon Crystal. *Phys. Rev. Lett.* **102,** 055703 (2009).
34. Yao, Y. *et al.* Comment on New metallic carbon crystal. *Phys. Rev. Lett.* **102,** 229601 (2009).
35. Liang, Y., Zhang, W. & Chen, L. Phase stabilities and mechanical properties of two new carbon crystals. *Europhys. Lett.* **87,** 56003 (2009).
36. Martinez-Canales, M., Pickard, C. J. & Needs, R. J. Thermodynamically stable phases of carbon at multiterapascal pressures. *Phys. Rev. Lett.* **108,** 045704 (2012).
37. Zhang, S. H., Wang, Q., Chen, X. S. & Jena, P. Stable three-dimensional metallic carbon with interlocking hexagons. *PNAS.* **110,** 18809–18813 (2013).
38. Niu, C. Y., Wang, X. Q. & Wang, J. T. K_6 carbon: A metallic carbon allotrope in sp^3 bonding networks *J. Chem. Phys.* **140,** 054514 (2014).
39. Perdew, J. P. & Zunger, A. Self-interaction correction to density-functional approximations for many-electron systems. *Phys. Rev. B* **23,** 5048 (1981).
40. Perdew, J. P., Burke, K. & Ernzerhof, M. Generalized gradient approximation made simple. *Phys. Rev. Lett.* **77,** 3865 (1996).
41. Kresse, G. & Furthmüller, J. Efficient iterative schemes for *ab initio* total-energy calculations using a plane-wave basis set. *Phys. Rev. B* **54,** 11169 (1996).
42. Kresse, G. & Hafner, J. Efficiency of *ab-initio* total energy calculations for metals and semiconductors using a plane-wave basis set. *Comput. Mater. Sci.* **6,** 15–50 (1996).
43. Kresse, G. & Joubert, D. From ultrasoft pseudopotentials to the projector augmented-wave method. *Phys. Rev. B* **59,** 1758 (1999).
44. Blöchl, P. E. Projector augmented-wave method. *Phys. Rev. B* **50,** 17953 (1994).
45. Togo, A., Oba, F. & Tanaka, I. First-principles calculations of the ferroelastic transition between rutile-type and $CaCl_2$-type SiO_2 at high pressures. *Phys. Rev. B* **78,** 134106 (2008).
46. Togo, A. Phonopy, http://phonopy.sourceforge.net/.
47. Pantea, D., Brochu, S., Thiboutot, S., Ampleman, G. & Schol, G. A morphological investigation of soot produced by the detonation of munitions. *Chemosphere* **65,** 821–831 (2006).
48. Yin, M. T. Si-1 (BC-8) crystal phase of Si and C: Structural properties, phase stabilities, and phase transitions. *Phys. Rev. B* **30,** 1773–1776 (1984).
49. Johnston, R. L. & Hoffmann, R. Superdense carbon, C8: supercubane or analog of γ-silicon ? *J. Am. Chem. Soc.* **111,** 810–819 (1989).
50. Knudson, M. D., Desjarlais, M. P. & Dolan, D. H. Shock-wave exploration of the high-pressure phase of carbon. *Science* **322,** 1822–1825 (2004).
51. Ward, A., Broido, D. A., Stewart, D. A. & Deinzer, G. *Ab initio* theory of the lattice thermal conductivity in diamond *Phys. Rev. B* **80,** 125203 (2009).
52. Maultzsch, J., Reich, S., Thomsen, C., Requardt, H. & Ordejón, P. Phonon dispersion in graphite. *Phys. Rev. Lett.* **92,** 075501 (2004).
53. Mouhat, F. & Coudert, F. X. Necessary and sufficient elastic stability conditions in various crystal systems. *Phys. Rev. B* **90,** 224104 (2014).
54. Hill, R. The elastic behaviour of a crystalline aggregate. *Proc. Phys. Soc.* (London) **65,** 350 (1952).
55. Pugh, S. F. Relations between the elastic moduli and the plastic properties of polycrystalline pure metals. *Philos.Mag.* **45,** 823–843 (1954).
56. Ferrari, A. C. *et al.* Raman spectrum of graphene and graphene layers. *Phys. Rev. Lett.* **97,** 187401 (2006).
57. Kobashi, K., Nishimura, K., Kawate, Y. & Horiuchi, T. Synthesis of diamonds by use of microwave plasma chemical-vapor deposition: morphology and growth of diamond films. *Phys. Rev. B* **38,** 4067 (1988).
58. Heyd, J., Scuseria, G. E. & Ernzerhof, M. Hybrid functionals based on a screened coulomb potential. *J. Chem. Phys.* **118,** 8207 (2003).
59. Heyd, J., Scuseria, G. E. & Ernzerhof, M. Erratum: Hybrid functionals based on a screened coulomb potential. *J. Chem. Phys.* 124, 219906 (2006).
60. Nose, S. A unified formulation of the constant temperature molecular dynamics methods. *J. Chem. Phys.* **81,** 511C519 (1984).

Acknowledgements

This work is supported by the Specialized Research Fund for the Doctoral Program of Higher Education of China (Grant No.20114101110001), the NSFC of China (Grant No. 11504332 and 11274280), the China Postdoctoral Science Foundation (2015M580633) and the National Basic Research Program of China (No. 2012CB921300); Jian-Tao Wang acknowledges support from the NSFC of China (Grant No. 11274356) and the Strategic Priority Research Program of the Chinese Academy of Sciences (Grant No. XDB07000000). Jun-Hyung Cho acknowledges support from National Research Foundation of Korea (Grant No. 2015R1A2A2A01003248).

Author Contributions

C.Y.N., C.X.Z., J.H.C., Y.J. and J.T.W. designed the study and wrote the paper; C.Y.N. and C.X.Z. carried out first-principles simulations; Z.J.Q. and X.Y.R. participated in writing of the manuscript; all authors discussed the results and contributed to the manuscript.

Additional Information

Competing financial interests: The authors declare no competing financial interests.

How to cite this article: Zhao, C.-X. *et al.* H_{18} Carbon: A New Metallic Phase with sp^2-sp^3 Hybridized Bonding Network. *Sci. Rep.* **6**, 21879; doi: 10.1038/srep21879 (2016).